Superfluid Bose-Fermi mixture with spin-orbit coupling

Liang-Liang Wang [1,2] Wenjun Shao [1,2,3] Qing Sun,[4] and Jian Li[1,2,*]

[1]*School of Science, Westlake University, 18 Shilongshan Road, Hangzhou 310024, Zhejiang Province, China*

[2]*Institute of Natural Sciences, Westlake Institute for Advanced Study, 18 Shilongshan Road, Hangzhou 310024, Zhejiang Province, China*

[3]*Westlake Institute for Advanced Study, Fudan University, Shanghai 200433, China*

[4]*Department of Physics, Capital Normal University, Beijing 100048, China*

(Received 22 December 2022; accepted 10 March 2023; published 24 March 2023)

We investigate a fermionic superfluid with Raman-induced spin-orbit coupling immersed in a Bose-Einstein condensate. By minimizing the total free energy, we find that, with moderate repulsive interspecies interaction, a phase separation occurs where the otherwise nontopological uniform phase is divided into two parts: a purely fermionic one and a Bose-Fermi mix characterized by nontrivial topology with the winding number $W = 1$. We verify that Majorana zero modes emerge at the phase interfaces by numerical simulations of the coupled Bogoliubov–de Gennes and Gross–Pitaevskii equations in real space. The tunability of the phase interfaces enables a direct manipulation of the predicted Majorana zero modes.

DOI: 10.1103/PhysRevA.107.033326

I. INTRODUCTION

The mixture of binary superfluids belonging to different statistics, is a long standing research topic in the context of quantum superfluids. However, the unique mixture of superfluid bosonic ^{4}He and fermionic ^{3}He [1,2], which is predicted to undergo a transition between *s*-wave and *p*-wave Cooper pairs, is still out of reach with currently available cryogenic techniques. Excitingly, superfluid Bose-Fermi mixtures (BFMs) in ultracold atomic gases, where bosons form a weakly interacting Bose-Einstein condensate (BEC) and fermions form a Bardeen-Cooper-Schrieffer (BCS) superfluid, have been realized by using the combination of the Feshbach resonance and radio-frequency techniques [3–7]. The experimental breakthrough completely changes the objective of studying superfluid mixtures and has drawn lots of theoretical attention recently [8–24]. Many fascinating behaviors due to the interaction between bosons and fermions have been predicted, including mixing-demixing transitions [8], dark-bright solitons [9], vortex lattice reformation [10], and coupled dipole oscillation [13,15] the or enhanced Fulde-Ferrell-Larkin-Ovchinnikov state [19].

In recent years, we have witnessed outstanding progress in experimental realization of spin-orbit (SO) coupling of ultracold atoms [25–30]. SO coupling in ultracold atom physics arises from a synthetic gauge field created by the interaction between atoms and the Raman laser field. It significantly changes the Fermi surface and makes nontrivial topological phases and relevant intriguing phenomena all possible [31–39]. However, most of the previous theoretical and experimental studies on binary superfluids, were concentrating either on BFMs composed by nontopological superfluids, or on the mixtures with two species belonging to same statistics [40–46]. Topological phases and topological protected excitations: Majorana zero modes with non-Abelian exchange statistics [47] in superfluid BFMs, have been less investigated. Apart from giving rise to the exhibition of fully phase-separated states [48], the interaction between bosons and fermions also causes robust self-induced density modulations, and incidental phase interfaces might host Majorana zero modes. Therefore, it is a natural step to bring these two exciting developments together and consider BFMs of ultracold atomic gases with SO coupling.

The goal of this paper is to study a fermionic superfluid with Raman-induced SO coupling immersed in a BEC and address the question of how the interaction between bosons and fermions affect the topological property of BFMs. By minimizing the total free energy of the system, we observe that, once the repulsive interspecies interaction is brought close to the fully phase-separation point, the uniform BFM becomes unstable and exhibits a purely fermionic phase coexisting with a mixed one. Due to the effect of SO coupling, the system consists of both nontopological and topological phase and the phase interfaces are predicted to host Majorana zero modes. The topology of distinct phases are verified by the winding number and better understood by observing the close and reopen of the excitation gap. We further give reliable results by self-consistently solving the coupled Bogoliubov–de Gennes and Gross–Pitaevskii (BdG-GP) equations in real space, and present the emergence of Majorana zero modes at the phase interfaces. In addition, the change of atomic ratio or interspecies interaction shifts the position of the phase interfaces and therefore can be used for tuning Majorana zero modes. The Majorana zero modes at the phase interfaces should leave signatures in the spatially resolved radio-frequency spectroscopy, which, in principle, can be detected using existing experimental techniques.

The paper is organized as follows: In Sec. II, we describe the quasi-one-dimensional (1D) model used in our

*lijian@westlake.edu.cn

 ©2023 American Physical Society

investigation and obtain the total free energy with the introduction of the order parameters for fermions and wave functions for bosons. Section III presents the possible phases in superfluid BFM with SO coupling and determines the phase transition by minimizing the total free energy. In Sec. IV we restrict the system in a tight waveguide and give reliable results by self-consistently solving the coupled BdG-GP equations for the observation of the associated Majorana zero modes at the phase interfaces. Finally, in Sec. V we present a discussion and conclusion of our study.

II. MODEL

We consider a two-component Fermi gas with Raman-induced SO coupling immersed in a weakly interacting BEC. The Raman dressing scheme is based on coupling two atomic internal hyperfine states of the fermions with two counter-propagating Raman lasers [26]. The mixture in which both fermionic and bosonic species are superfluids is confined in a toroidal trap with tight cylindrically symmetric harmonic confinement of frequency $\omega_\perp$ in the transverse direction. The atoms have an effective quasi-1D behavior if the chemical potentials are much smaller than the transverse energy $\hbar\omega_\perp$ [49]. The effective Hamiltonian for the superfluid BFM can be written as

$$\begin{aligned}\hat{H} = &\int dx \hat{\psi}_{\rm f}^\dagger [H_{\rm s}(x) - \mu_{\rm f}]\hat{\psi}_{\rm f} + g_{\rm f}\hat{\psi}_\uparrow^\dagger \hat{\psi}_\downarrow^\dagger \hat{\psi}_\downarrow \hat{\psi}_\uparrow \\ &+ \int dx \hat{\psi}_{\rm b}^\dagger \left[-\hbar^2\partial_x^2/2m_{\rm b} - \mu_{\rm b}\right]\hat{\psi}_{\rm b} + g_{\rm b}\hat{\psi}_{\rm b}^\dagger \hat{\psi}_{\rm b}^\dagger \hat{\psi}_{\rm b}\hat{\psi}_{\rm b} \\ &+ \int dx g_{\rm bf}\hat{\psi}_{\rm b}^\dagger \hat{\psi}_{\rm b}\hat{\psi}_{\rm f}^\dagger \hat{\psi}_{\rm f}, \end{aligned} \tag{1}$$

where $\hat{\psi}_{\rm f} \equiv [\hat{\psi}_\uparrow, \hat{\psi}_\downarrow]^T$ denotes the field operator for fermions with pseudospins and $\hat{\psi}_{\rm b}$ is the bosonic field operator. $H_{\rm s}(x) = -\hbar^2\partial_x^2/2m_{\rm f} + i\alpha\sigma_y\partial_x - h_z\sigma_z$ is the single-particle Hamiltonian of fermionic atoms, which has a general form of Raman-induced SO coupling with strength α. x is the spatial coordinate along the circumference (of length L). h_z is the effective Zeeman field. The bosonic and fermionic components cannot be transformed into each other, each of both has its own chemical potential $\mu_{\rm f}$ ($\mu_{\rm b}$). The interaction between atoms are given in terms of corresponding scattering lengths: $g_{\rm b} = 2\hbar\omega_\perp a_{\rm b}$, $g_{\rm f} = 2\hbar\omega_\perp a_{\rm f}$, and $g_{\rm bf} = 2\hbar\omega_\perp a_{\rm bf}$.

With the introduction of the order parameter $\Delta(x) = -g_{\rm f}\langle\hat{\psi}_\downarrow\hat{\psi}_\uparrow\rangle$ for fermions and wave function $\psi_{\rm b}(x) = \langle\hat{\psi}_{\rm b}\rangle$ for bosons, the free-energy density of a uniform superfluid BFM with SO coupling can be obtained as

$$\mathcal{E}[n_{\rm b}, n_{\rm f}] = g_{\rm b}n_{\rm b}^2 + \sum_{\mathbf{k}} \xi_{|-\mathbf{k}|} + \sum_{\mathbf{k},\nu} \Theta\left(-E_{\mathbf{k},\nu}^\eta\right)E_{\mathbf{k},\nu}^\eta - \frac{|\Delta|^2}{g_{\rm f}}, \tag{2}$$

where $n_{\rm f} = \sum_\sigma \langle\hat{\psi}_\sigma^\dagger\hat{\psi}_\sigma\rangle$ and $n_{\rm b} = |\psi_{\rm b}|^2$ are respectively the fermion and boson densities. The kinetic energy of the bosons vanishes and $\xi_{\mathbf{k}} = \hbar^2\mathbf{k}^2/2m_{\rm f} + g_{\rm bf}n_{\rm b} - \mu_{\rm f}$. In Eq. (2), $\Theta(x)$ is the Heaviside step function. The quasiparticle ($\eta = +$) and quasihole ($\eta = -$) dispersions $E_{\mathbf{k},\nu}^\eta (\nu = 1, 2)$ are the eigenvalues of the Bogoliubov–de Gennes (BdG) matrix

$$H_{\rm BdG} = \begin{pmatrix} \xi_{\mathbf{k}} - h_z & -i\alpha\mathbf{k} & 0 & \Delta \\ i\alpha\mathbf{k} & \xi_{\mathbf{k}} + h_z & -\Delta & 0 \\ 0 & -\Delta^* & -\xi_{-\mathbf{k}} + h_z & i\alpha\mathbf{k} \\ \Delta^* & 0 & -i\alpha\mathbf{k} & -\xi_{-\mathbf{k}} - h_z \end{pmatrix} \tag{3}$$

under the Numbu spinor basis $[\hat{\psi}_{\uparrow,\mathbf{k}}, \hat{\psi}_{\downarrow,\mathbf{k}}, \hat{\psi}_{\uparrow,-\mathbf{k}}^\dagger, \hat{\psi}_{\downarrow,-\mathbf{k}}^\dagger]^T$. Without loss of generality, we assume h_z, α, and Δ to be real and $m_{\rm b} = m_{\rm f} = m$ throughout the work. This could be approximated well in the BFMs ^{7}Li - ^{6}Li as well as ^{39}K - ^{40}K of experimental interest. The order parameter and chemical potential are determined self-consistently by solving the following conditions: $\partial\mathcal{E}/\partial\Delta = 0$, $n_{\rm f} = -\partial\mathcal{E}/\partial\mu_{\rm f}$.

As was done in Ref. [49] for an ideal spin-polarized Fermi gas interacting with a dilute Bose gas, we now analyze the general phase stability of superfluid BFM by a binary mixture which can have at most two distinct phases. Here we use subscripts $i = 1, 2$ to label the physical quantities specific to each. The volume fractions of the phases are $l_1 = L_1/L$ and $l_2 = 1 - l_1$, then the total free-energy density for the phase-separated mixture is $\mathcal{E} = \sum_{i=1,2} l_i\mathcal{E}_i$. There are four possible existences of phase: (i) a uniform mixture, where both components occupy the entire space at constant densities; (ii) a fully separated phase where fermions and bosons are completed separated; and a partially separated phase, where (iii) part of the space is occupied by fermions (bosons) and (iv) partly by a Bose-Fermi mix. Here we note that the topological properties of different regions are determined by the winding number, respectively [45]. For the fixed total densities $l_1 n_{\rm b(f),1} + l_2 n_{\rm b(f),2} = n_{\rm b(f)}$, the allowed parameters $(l_1, n_{\rm b(f),1}, n_{\rm b(f),2})$ as well as the pairing order parameters $\Delta_{1,2}$ can then be determined by the principle of minimum energy with $\mu_{\rm f,1} = \mu_{\rm f,2}$. It is convenient to work in terms of dimensionless variables defined in terms of Fermi wave vector $k_{\rm f} \equiv \pi n_{\rm f}/2$ and Fermi energy $E_{\rm f} \equiv \hbar^2 k_{\rm f}^2/2m_{\rm f}$ by $\psi_b = \sqrt{k_{\rm f}}\tilde{\psi}_b$, $g_j = \tilde{g}_j\hbar^2 k_{\rm f}/(2m_{\rm f})$, $h_z = \tilde{h}_z E_{\rm f}$, $\Delta = \tilde{\Delta}E_{\rm f}$, and $\alpha = \tilde{\alpha}\hbar^2 k_{\rm f}/(2m_{\rm f})$.

III. TOPOLOGICAL PHASE SEPARATION

Our calculations indicate that topological phase separation can occur under suitable interspecies interaction. By minimizing the total free energy, we plot the change of volume fractions l_i [Fig. 1(a)] along with the order parameters $|\Delta_i|$ [Fig. 1(b)], the atomic density $n_{\rm b,f,}i$ [Fig. 1(c)], and the winding numbers W_i [Fig. 1(d)] with subscripts $i = 1, 2$ as a function of interspecies interaction $g_{\rm bf}$ in Fig. 1. Here we note that the system is prepared in a topological trivial state with no interspecies interaction $g_{\rm bf} = 0$. According to the results of Figs. 1(a) and 1(c), an apparent conclusion can be drawn that, in superfluid BFMs with SO coupling, only three phases are supported: a uniform mixture with $l_2 = 0$, a fully separated phase with $n_{\rm b,1}n_{\rm f,1} = n_{\rm b,2}n_{\rm f,2} = 0$, and a partially separated phase, where a mixed phase surrounded by pure fermions. With increasing $g_{\rm bf}$, the uniform phase gets unstable and then displays a self-induced localization of bosons in the fermion density profiles. Such self-induced localization lowers the fermionic density but does not destroy the bulk gap of BCS superfluid. Finally, a strong $g_{\rm bf}$ produces a fully separated

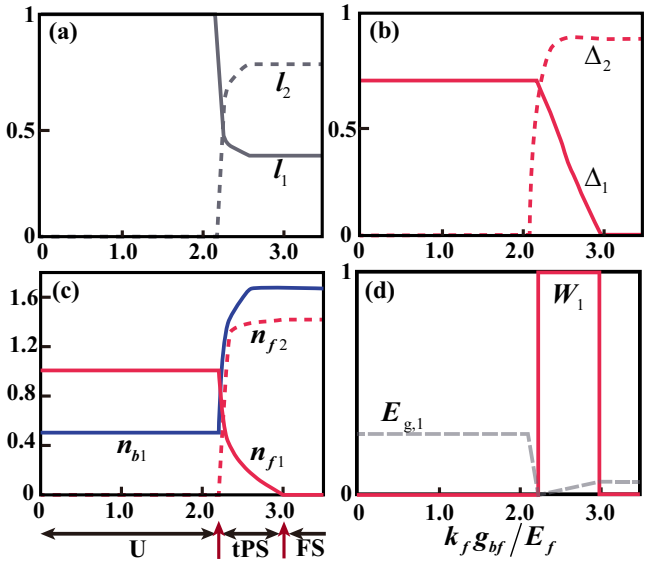

FIG. 1. (a) The volume fractions, (b) order parameters, (c) atomic densities, and (d) corresponding winding numbers of the phases $i = 1, 2$ as functions of interspecies interaction $g_{\rm bf}$. The arrows label the transitions from the uniform mixture (U) to the topological partially separated phase (tPS), and tPS to the fully separated phase (FS), as shown in panel (c). The topological properties are determined by the winding number W_1 and the bulk quasiparticle excitation gap $E_{g,1} = 2|h_z - (\mu_1^2 + \Delta_1^2)^{1/2}|$ shown in panel (d). Here, we have taken $\alpha = 1E_{\rm f}/k_{\rm f}$, $k_{\rm f} g_{\rm b} = 1E_{\rm f}$, $k_{\rm f} g_{\rm f} = 3E_{\rm f}$, $h_z = 1.0E_{\rm f}$, and $n_{\rm b} = 0.5$.

phase, and these effects are clearly shown in Fig. 1(c), where we plot the density profiles. It is worth noticing that a Bose-Bose mixture only admits the uniform phase and the fully separated phase.

To further explore the transition from nontopological to topological phases, we have calculated the winding numbers of the Fermi superfluids, which is necessary to the change of the topology. From Fig. 1(d), the system evolves from nontopological phase ($W_1 = 0$) to a topological state ($W_1 = 1$) when it enters the partially separated phase. The winding number W_2 is always zero and hence is not depicted. Thus we have a mixed phase with both nontopological and topological superfluid components, which separate from each other spatially. Here we give the phase its name–"topological partially separated phase" (tPS). To better understand the transition from nontopological to topological phases, we further observe the closing and reopening of the bulk quasiparticle excitation gaps, which is determined by $E_{{\rm g},i} = 2|h_z - (\mu_i^2 + \Delta_i^2)^{1/2}|$ with $\mu_i = \mu - g_{\rm bf} n_{{\rm b}i}$. Thus, the transition occurs at the Zeeman field threshold $h_{c,i} = (\mu_i^2 + \Delta_i^2)^{1/2}$ and the system will be in a conventional superfluid state at $h_z < h_{c,i}$ and in a topological superfluid state at $h_z > h_{c,i}$. The Majorana zero-energy modes are expected to appear at the phase interfaces between those two distinct phases.

IV. MAJORANA ZERO-MODES AT THE PHASE INTERFACE

To observe the Majorana zero modes at the phase interfaces, we restricted the system in a atomic waveguide, i.e., a finite quasi-1D cylinder with the trap $V(x) = 0$ $(-L/2 < x < L/2)$ and $V(x) = \infty$ (otherwise). The axial length L of the atomic waveguide is much larger than the transverse width. In this case, we can derive the generalized BdG equation in real space from Eq. (3) by $\mathbf{k} \to -i\hbar\partial/\partial_x$ for fermions: $H_{\rm BdG}(x)\Psi_\eta(x) = E_\eta \Psi_\eta(x)$, where $\Psi_\eta(x) \equiv [u_{\uparrow,\eta}(x), u_{\downarrow,\eta}(x), v_{\uparrow,\eta}(x), v_{\downarrow,\eta}(x)]^T$ are the Numbu spinor wave functions corresponding to the quasiparticle excitation energy E_η. It is coupled to the GP equation for bosons:

$$\left[-\frac{\hbar^2}{2m_{\rm b}}\partial_x^2 + g_{\rm bf} n_{\rm f} + V(x) + g_{\rm b}|\psi_{\rm b}|^2\right]\psi_{\rm b} = \mu_{\rm b}\psi_{\rm b}. \quad (4)$$

The order parameter $\Delta(x)$ and the chemical potential $\mu_{\rm f}$ in the real-space BdG equation can be determined self-consistently with

$$\Delta(x) = -\frac{g_{\rm f}}{2}\sum_\eta [u_\uparrow(x)v_\downarrow^*(x)f(E_\eta) + u_\downarrow(x)v_\uparrow^*(x)f(-E_\eta)] \quad (5)$$

and the number equation $N_{\rm f} = \int dx[n_\uparrow(x) + n_\downarrow(x)]$ with

$$n_\sigma(x) = \frac{1}{2}\sum_\eta [|u_\sigma(x)|^2 f(E_\eta) + |v_\sigma(x)|^2 f(-E_\eta)] \quad (6)$$

being the local density of σ fermions. $f(E) = 1/[e^{E/(k_B T)}+1]$ is the Fermi distribution function at temperature T. The coupled real-space BdG-GP equations are solved by means of an iterative procedure, which starts from a trial function $\Delta(x)$, $\psi_{\rm b}(x)$, $\mu_{\rm f}$ and converges to the self-consistent solutions. In each procedure, we solve the BdG equation following the basis expansion method in Ref. [50] and GP equation by using an imaginary-time propagation method based on the finite-difference Crank-Nicholson discretization scheme [51]. For our numerical calculations, we consider a superfluid BFM with fixed total numbers of fermions $N_{\rm f} = 100$ and of bosons $N_{\rm b} = 10$ confined in a tight waveguide of size $L = 50k_{\rm f}/\pi$. In the finite-difference discretization we use a space step of 0.001 and time step of 0.0005. An energy cutoff $E_c = 10E_{\rm f}$ is adopted, which is found to be large enough to ensure the numerical accuracy. All calculations are done under zero temperature $T = 0$.

In Fig. 2, three results with different values of $g_{\rm bf}$ are chosen as representation of the typical phases predicted in the Sec. III. First, let us concentrate on the left column where we plot the density profiles of bosons (red line) and fermions (blue lines), respectively. For the zero value of $g_{\rm bf}$, there is no connection between bosons and fermions and both of them are evenly distributed. With increasing $g_{\rm bf}$, the bosonic and fermionic gases, especially the spin-down component, tend to separate from each other and create a potential well in their vicinity, as shown in the middle panel. Clearly, the localization effect is the result of boson-fermion interactions. It relies on a local deformation of the density of fermions and is not effected by the boundary conditions. For sufficiently strong boson-fermion interaction, bosonic and fermionic gases are fully separated: bosons are localized in a small area and fermions are rejected to both sides of the area. The appearance of the topological phase can be simply monitored by the calculation of $h_z - h_c(x)$. The local uniform cell will be

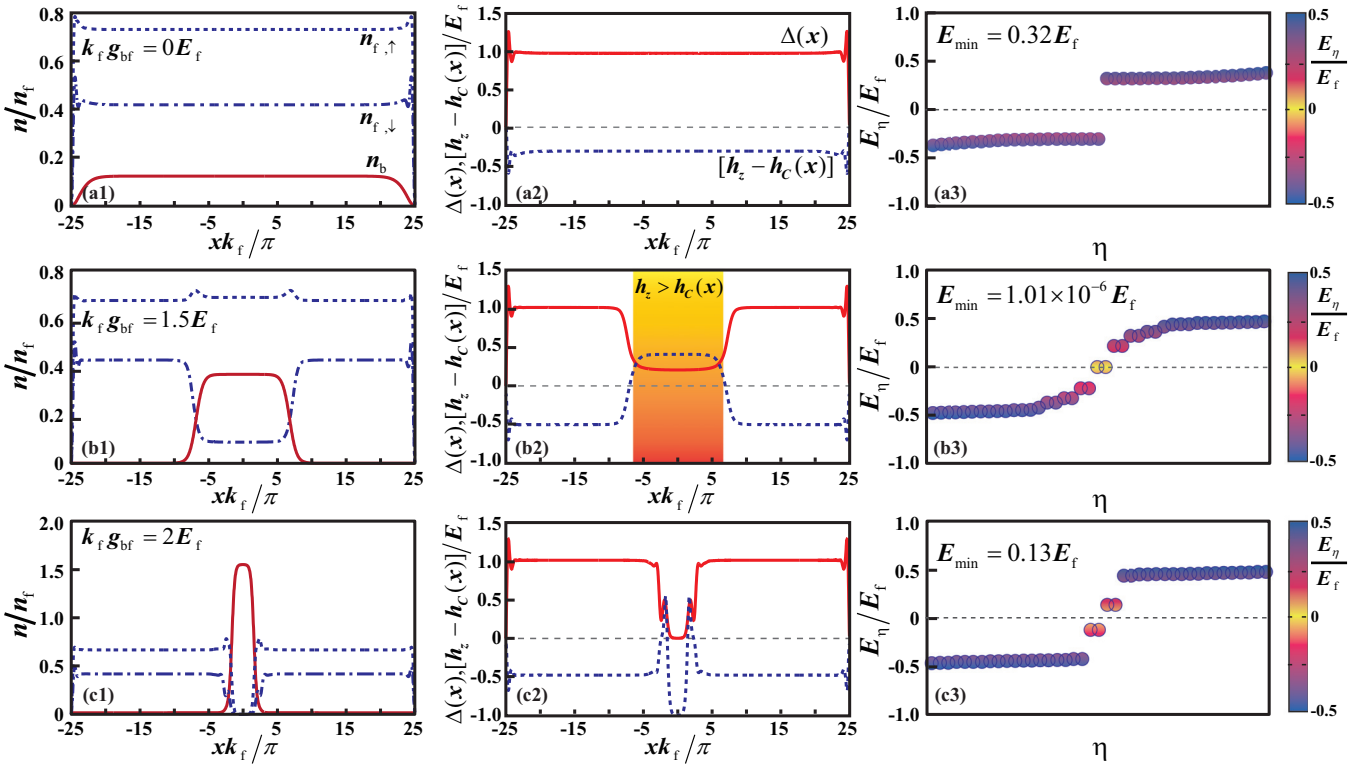

FIG. 2. (left column) Density profiles of the fermions and bosons for three sets of interaction parameters. (middle column) The order parameter $\Delta(x)$ of the Fermi superfluid and the spatial distribution of $h_z - h_c(x)$ for the same configurations as the left column. The area in which the fermionic atoms are in the topological superfluid state is highlighted by the yellow colors. The right column show the behavior of the eigenenergy spectrums at these three interactions: $k_f g_{bf} = 0E_f$, $1.5E_f$, and $2.0E_f$, respectively. Here $\alpha = E_f/k_f$, $k_f g_f = 3E_f$, $h_z = 1E_f$, and $k_f g_b = 2E_f$.

in the topological state if $h_z > h_c(x)$. This is demonstrated in the center column of Fig. 2, where we plot the order parameter and the spatial distribution of $h_z - h_c(x)$. Without the boson-fermion interaction, $h_z < h_c(x)$ for any position x and the whole fermionic gas is in the conventional superfluid. In the case of topological partially separated phase (middle column in Fig. 2), the order parameter $\Delta(x)$ reduces in the middle of the potential where $h_z > h_c(x)$ is satisfied. The area of topological superfluid is highlighted by the yellow colors. At a large boson-fermion interaction $g_{bf} = 2.0E_f/k_f$, bosons and fermions are completed separated and the condition $h_z < h_c(x)$ extends over the whole system. As shown in the right column of Fig. 2, the behavior of the quasiparticle energy spectrum can clearly reveal the emergence of Majorana zero modes.

The wave functions of the Majorana zero modes in the middle panel of Fig. 2 are shown in Fig. 3. In this example, we can see that the wave functions readily satisfy either $u_{j,\sigma}(x) = v^*_{j,\sigma}(x)$ or $u_{j,\sigma}(x) = -v^*_{j,\sigma}(x)$, meeting the requirement of the self-Hermitian condition for Majorana fermions. The overlap between the wave functions at the phase boundaries $xk_f/\pi \approx \pm 7$ lead to finite but exponentially small energy splitting: $E_{zes} \approx \pm 1.10 \times 10^{-6} E_f$. A practice way to probe the Majorana zero modes is to measure the local density of states (LDoS) using the spatially resolved radio-frequency (rf) spectroscopy [52], with which we anticipate that the contribution of Majorana fermions will be well isolated in both energy domain and real space. The local density of states for spin-up and spin-down atoms is defined by $\rho_\sigma(x, E) = 1/2 \sum_\eta [|u_{\sigma,\eta}|^2 \delta(E - E_\eta) + |v_{\sigma,\eta}|^2 \delta(E + E_\eta)]$. In Fig. 4, we show that the local density of states $\rho_\sigma(x, E)$ and the contribution from Majorana zero modes are clearly visible near zero energy and well isolated from other quasiparticle contributions by an energy gap $\Delta \approx 0.3E_f$. There are two Majorana

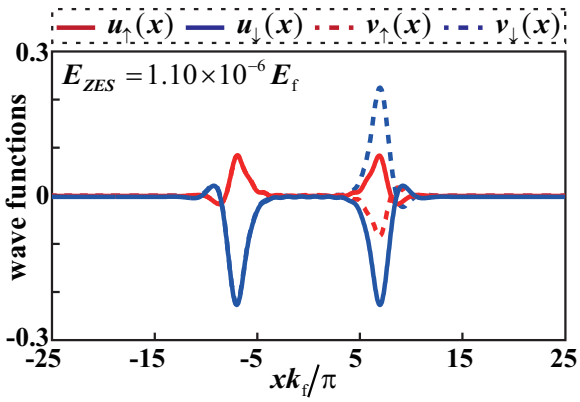

FIG. 3. Wave functions of Majorana zero modes. Due to the intrinsic symmetry $u^+_{\sigma\eta} \to v^{-*}_{\sigma\eta}$ with $E_\eta \to -E_\eta$, where $\pm$ refer to quasiparticle and hole excitations, we just show the wave functions of quasiparticle zero modes. The modes satisfy the symmetry requirement for Majorana zero modes $u_\sigma(x) = v^*_\sigma(x)$ or $u_\sigma(x) = -v^*_\sigma(x)$. The parameters are the same as the case of the middle panel in Fig. 2.

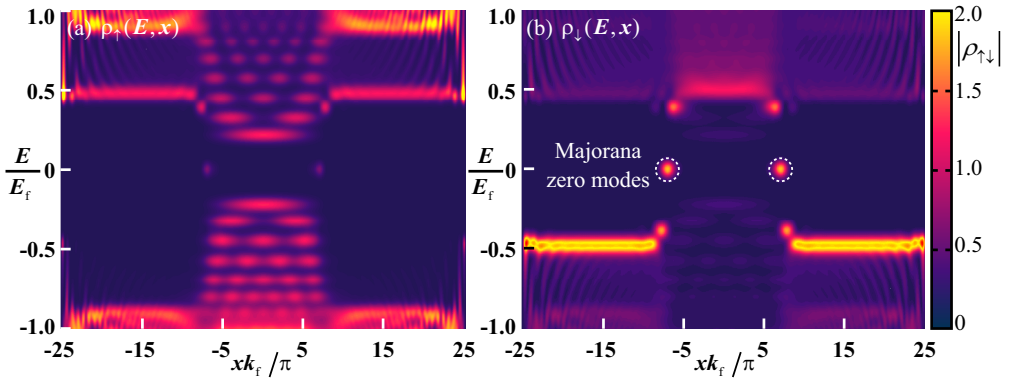

FIG. 4. Linear contour plot for the local density of states of spin-up atoms $\rho_\uparrow(x, E)$ and of spin-down atoms $\rho_\downarrow(x, E)$ for the case in Fig. 3. The signals of Majorana zero modes are well isolated in the energy and spatial domain, which are highlighted by white circles.

induced zero-energy peaks at $xk_f \approx \pm 7$ as shown in Fig. 4. Note that the Majorana zero modes mainly contributed to $\rho_\downarrow(x, E)$.

To gain more information, we preform calculation for several values of the atomic ratio $\gamma = N_f/N_b$, and we observe the change of the position of phase interfaces and movement of the associated Majorana zero modes. In Fig. 5, the density distribution and order parameter are reported for three values of γ. With increasing atomic ratio, in other words, adding more boson atoms, we observe that the topological phase area spread out while keeping the same structure of the topological interfaces. It suggests the Majorana zero modes at the phase interfaces move away from each other, thus providing a direct manipulation of the Majorana zero modes.

V. CONCLUSION

In this work we investigate the novel topological properties of superfluid BFMs with SO coupling and carefully study both the homogeneous behavior and the spatial behavior of the system in real space with reflective boundaries. We tune the interaction between bosons and fermions and, by minimizing the total free energy, explore three possible phase regimes of uniform, partially separated and fully separated phases. In our case, the phase separation is induced by the self-incurred localization of particles, not by the confining trap. The focus of the work is on the regime of partially separated phase, and we find that, two distinct uniform regions of fermions, both nontopological and topological phase, can coexist in the system. They are characterized by the different winding numbers and the emergence of Majorana zero modes is predicted at the phase interfaces. This mechanism distinguishes our work from most of the previous scenarios with phase separations. We further give reliable results by self-consistently solving the coupled BdG-GP equations and demonstrate the evident signals of Majorana zero modes at the phase interfaces in real space. Moreover, the change of atomic ratio or interspecies interaction shifts the position of the phase interfaces and associated Majorana zero modes, thus providing more knobs for tuning the Majorana zero modes. In view of the recent

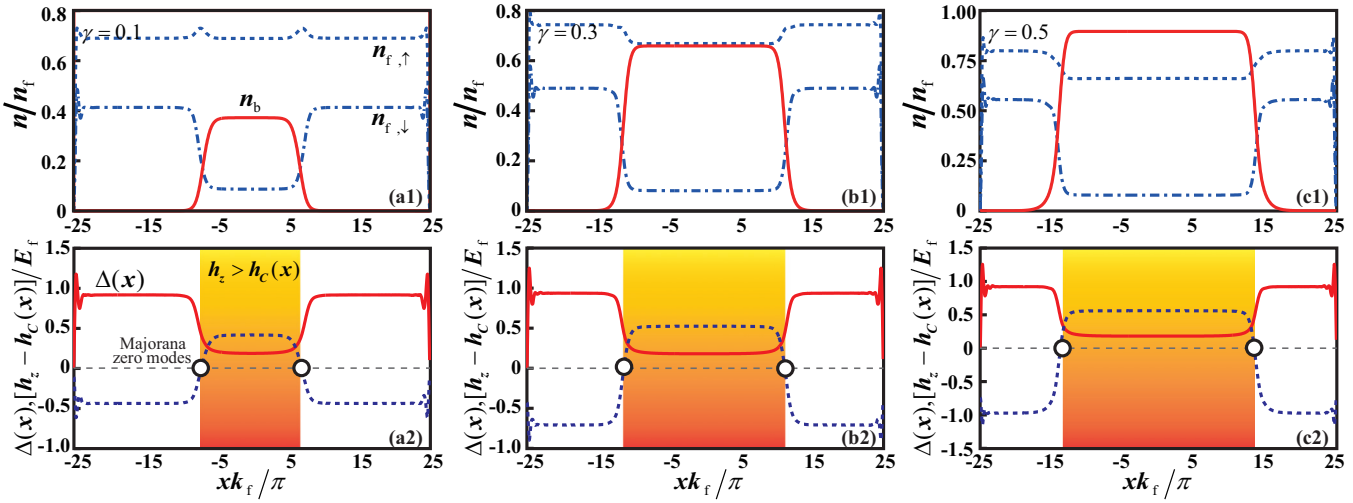

FIG. 5. (upper panel) Density profiles of the fermions and bosons for three sets of atomic ratios. (bottom panel) The order parameter $\Delta(x)$ of the Fermi superfluid and the spatial distribution of $h_z - h_c(x)$ for different atomic ratios. The area in which the fermionic atoms are in the topological superfluid state is highlighted by the yellow colors. the white circles denote Majorana zero modes. The other parameters are the same as the case in Fig. 2.

realization of the superfluid BFMs, our theoretical predication can be verified experimentally in the near future.

ACKNOWLEDGMENTS

We would like to thank Changan Li and Yong Sun for interesting discussions. This work was supported by NSFC under Grants No. 11875195 and No. 11474205, foundation of Beijing Education Committees under Grants No. CITTCD201804074, and No. KZ201810028043, and foundation of Zhejiang Province Natural Science under Grant No. LQ20A040002. J.L. acknowledges support from National Natural Science Foundation of China under Project No. 11774317. The numerical calculations in this paper have been done on the supercomputing system in the Information Technology Center of Westlake University.

[1] C. Ebner and D. Edwards, The low temperature thermodynamic properties of superfluid solutions of ^{3}He in ^{4}He, Phys. Rep. **2**, 77 (1971).

[2] D. Edwards and M. Pettersen, Lectures on the properties of liquid and solid ^{3}He - ^{4}He mixtures at low temperatures, J. Low Temp. Phys. **87**, 473 (1992).

[3] I. Ferrier-Barbut, M. Delehaye, S. Laurent, A. T. Grier, M. Pierce, B. S. Rem, F. Chevy, and C. Salomon, A mixture of Bose and Fermi superfluids, Science **345**, 1035 (2014).

[4] M. Delehaye, S. Laurent, I. Ferrier-Barbut, S. Jin, F. Chevy, and C. Salomon, Critical Velocity and Dissipation of an Ultracold Bose-Fermi Counterflow, Phys. Rev. Lett. **115**, 265303 (2015).

[5] X. C. Yao, H. Z. Chen, Y. P. Wu, X. P. Liu, X. Q. Wang, X. Jiang, Y. J. Deng, Y. A. Chen, and J. W. Pan, Observation of Coupled Vortex Lattices in a Mass-Imbalance Bose and Fermi Superfluid Mixture, Phys. Rev. Lett. **117**, 145301 (2016).

[6] R. Roy, A. Green, R. Bowler, and S. Gupta, Two-Element Mixture of Bose and Fermi Superfluids, Phys. Rev. Lett. **118**, 055301 (2017).

[7] B. DeSalvo, K. Patel, J. Johansen, and C. Chin, Observation of a Degenerate Fermi Gas Trapped by a Bose-Einstein Condensate, Phys. Rev. Lett. **119**, 233401 (2017).

[8] S. K. Adhikari and L. Salasnich, One-dimensional superfluid Bose-Fermi mixture: Mixing, demixing, and bright solitons, Phys. Rev. A **76**, 023612 (2007).

[9] M. Tylutki, A. Recati, F. Dalfovo, and S. Stringari, Dark-bright solitons in a superfluid Bose-Fermi mixture, New J. Phys. **18**, 053014 (2016).

[10] Y. Jiang, R. Qi, Z.-Y. Shi, and H. Zhai, Vortex Lattices in the Bose-Fermi Superfluid Mixture, Phys. Rev. Lett. **118**, 080403 (2017).

[11] J. S. Pan, W. Zhang, W. Yi, and G. C. Guo, Vortex-core structure in a mixture of Bose and Fermi superfluids, Phys. Rev. A **95**, 063614 (2017).

[12] J. M. Midtgaard, Z. Wu, and G. M. Bruun, Time-reversal-invariant topological superfluids in Bose-Fermi mixtures, Phys. Rev. A **96**, 033605 (2017).

[13] W. Wen and H. Li, Collective dipole oscillations in a mixture of Bose and Fermi superfluids in the BCS-BEC crossover, New J. Phys. **20**, 083044 (2018).

[14] L. Chen, C. Zhu, Y. Zhang, and H. Pu, Spin-exchange-induced spin-orbit coupling in a superfluid mixture, Phys. Rev. A **97**, 031601(R) (2018).

[15] Y. P. Wu, X. C. Yao, X. P. Liu, X. Q. Wang, Y. X. Wang, H. Z. Chen, Y. Deng, Y. A. Chen, and J. W. Pan, Coupled dipole oscillations of a mass-imbalanced Bose-Fermi superfluid mixture, Phys. Rev. B **97**, 020506(R) (2018).

[16] J. Kinnunen, Z. Wu, and G. Bruun, Induced *p*-Wave Pairing in Bose-Fermi Mixtures, Phys. Rev. Lett. **121**, 253402 (2018).

[17] C. Zhu, L. Chen, H. Hu, X. J. Liu, and Han Pu, Spin-exchange-induced exotic superfluids in a Bose-Fermi spinor mixture, Phys. Rev. A **100**, 031602(R) (2019).

[18] F. Kh. Abdullaev, M. Ögren, and M. P. Sørensen, Collective dynamics of Fermi-Bose mixtures with an oscillating scattering length, Phys. Rev. A **99**, 033614 (2019).

[19] M. Singh and G. Orso, Enhanced visibility of the Fulde-Ferrell-Larkin-Ovchinnikov state in one-dimensional Bose-Fermi mixtures near the immiscibility point, Phys. Rev. Res. **2**, 023148 (2020).

[20] M. Ögren and G. M. Kavoulakis, Rotational properties of superfluid Fermi-Bose mixtures in a tight toroidal trap, Phys. Rev. A **102**, 013323 (2020).

[21] K. Y. Jee and E. Mueller, Drag in Bose-Fermi mixtures, Phys. Rev. A **103**, 033307 (2021).

[22] O. I. Pâţu, Dynamical fermionization in a one-dimensional Bose-Fermi mixture, Phys. Rev. A **105**, 063309 (2022).

[23] J. C. Peacock, A. Ljepoja, and C. J. Bolech, Quantum coherent states of interacting Bose-Fermi mixtures in one dimension, Phys. Rev. Res. **4**, L022034 (2022).

[24] K. Hossain, S. Gupta, and Michael McNeil Forbes, Detecting entrainment in Fermi-Bose mixtures, Phys. Rev. A **105**, 063315 (2022).

[25] Y. Lin, K. Jiménez-García, and I. Spielman, Spin-orbit-coupled Bose-Einstein condensates, Nature (London) **471**, 83 (2011).

[26] P. Wang, Z. Yu, Z. Fu, J. Miao, L. Huang, S. Chai, H. Zhai, and J. Zhang, Spin-Orbit Coupled Degenerate Fermi Gases, Phys. Rev. Lett. **109**, 095301 (2012).

[27] Z. Wu, L. Zhang, W. Sun, X. Xu, B. Wang, S. Ji, Y. Deng, S. Chen, X. Liu, and J. Pan, Realization of two-dimensional spin-orbit coupling for Bose-Einstein condensates, Science **354**, 83 (2016).

[28] Z. Meng, L. Huang, P. Peng, D. Li, L. Chen, Y. Xu, C. Zhang, P. Wang, and J. Zhang, Experimental Observation of a Topological Band Gap Opening in Ultracold Fermi Gases with Two-Dimensional Spin-Orbit Coupling, Phys. Rev. Lett. **117**, 235304 (2016).

[29] L. Huang, Z. Meng, P. Wang, P. Peng, S.-L. Zhang, L. Chen, D. Li, Q. Zhou, and J. Zhang, Experimental realization of two-dimensional synthetic spin-orbit coupling in ultracold Fermi gases, Nat. Phys. **12**, 540 (2016).

[30] N. Q. Burdick, Y. Tang, and B. L. Lev, Long-Lived Spin-Orbit-Coupled Degenerate Dipolar Fermi Gas, Phys. Rev. X **6**, 031022 (2016).

[31] J. Dalibard, F. Gerbier, G. Juzeliūnas, and P. Öhberg, Colloquium: Artificial gauge potentials for neutral atoms, Rev. Mod. Phys. **83**, 1523 (2011).

[32] F. Wu, G. Guo, W. Zhang, and W. Yi, Unconventional Superfluid in a Two-Dimensional Fermi gas with Anisotropic Spin-Orbit Coupling and Zeeman fields, Phys. Rev. Lett. **110**, 110401 (2013).

[33] C. Qu, Z. Zheng, M. Gong, Y. Xu, L. Mao, X. Zou, G. Guo, and C. Zhang, Topological superfluids with finite-momentum pairing and Majorana fermions, Nat. Commun. **4**, 2710 (2013).

[34] W. Zhang and W. Yi, Topological Fulde-Ferrell-Larkin-Ovchinnikov states in spin-orbit-coupled Fermi gases, Nat. Commun. **4**, 2711 (2013).

[35] J. Devreese, J. Tempere, and C. Melo, Effects of Spin-Orbit Coupling on the Berezinskii-Kosterlitz-Thouless Transition and the Vortex-Antivortex Structure in Two-Dimensional Fermi Gases, Phys. Rev. Lett. **113**, 165304 (2014).

[36] H. Zhai, Degenerate quantum gases with spin-orbit coupling: A review, Rep. Prog. Phys. **78**, 026001 (2015).

[37] Z. Zheng, C. Qu, X. Zou, and C. Zhang, Fulde-Ferrell Superfluids without Spin Imbalance in Driven Optical Lattices, Phys. Rev. Lett. **116**, 120403 (2016).

[38] J. Li, J. Lee, W. Huang, S. Burchesky, B. Shteynas, F. To, A. Jamison, and W. Ketterle, A stripe phase with supersolid properties in spin-orbit-coupled Bose-Einstein condensates, Nature (London) **543**, 91 (2017).

[39] L. Wang, A. Ji, Q. Sun, and J. Li, Exotic Vortex States with Discrete Rotational Symmetry in Atomic Fermi Gases with Spin-Orbital-Angular-Momentum Coupling, Phys. Rev. Lett. **126**, 193401 (2021).

[40] M. Boninsegni, Phase Separation in Mixtures of Hard Core Bosons, Phys. Rev. Lett. **87**, 087201 (2001).

[41] P. Buonsante, S. Giampaolo, F. Illuminati, V. Penna, and A. Vezzani, Mixtures of Strongly Interacting Bosons in Optical Lattices, Phys. Rev. Lett. **100**, 240402 (2008).

[42] T. Keilmann, I. Cirac, and T. Roscilde, Dynamical Creation of a Supersolid in Asymmetric Mixtures of Bosons, Phys. Rev. Lett. **102**, 255304 (2009).

[43] T. Mishra, R. V. Pai, and B. P. Das, Induced supersolidity in a mixture of normal and hard-core Bosons, Phys. Rev. B **81**, 024503 (2010).

[44] L. L. Wang, Q. Sun, W. M. Liu, G. Juzeliūnas, and A. C. Ji, Fulde-Ferrell-Larkin-Ovchinnikov state to topological superfluidity transition in bilayer spin-orbit-coupled degenerate Fermi gases, Phys. Rev. A **95**, 053628 (2017).

[45] L. L. Wang, M. Gong, and W. M. Liu, Multiple Majorana zero modes in atomic Fermi double wires with spin-orbit coupling, Phys. Rev. A **96**, 023623 (2017).

[46] Q. Sun, L. L. Wang, X. J. Liu, G. Juzeliūnas, and A. C. Ji, Larkin-Ovchinnikov superfluidity in time-reversal-symmetric bilayer Fermi gases, Phys. Rev. A **99**, 043601 (2019).

[47] F. Wilczek, Majorana returns, Nat. Phys. **5**, 614 (2009).

[48] R. Lous, I. Fritsche, M. Jag, F. Lehmann, E. Krrilov, B. Huang, and R. Grimm, Probing the Interface of a Phase-Separated State in a Repulsive Bose-Fermi Mixture, Phys. Rev. Lett. **120**, 243403 (2018).

[49] K. Das, Bose-Fermi Mixtures in One Dimension, Phys. Rev. Lett. **90**, 170403 (2003).

[50] X. Liu, Soliton-induced Majorana fermions in a one-dimensional atomic topological superfluid, Phys. Rev. A **91**, 023610 (2015).

[51] S. K. Adhikari, Stabilization of bright solitons and vortex solitons in a trapless three-dimensional Bose-Einstein condensate by temporal modulation of the scattering length, Phys. Rev. A **69**, 063613 (2004).

[52] Y. Shin, C. Schunck, A. Schirotzek, and W. Ketterle, Tomographic rf Spectroscopy of a Trapped Fermi Gas at Unitarity, Phys. Rev. Lett. **99**, 090403 (2007).